

Controlled crystal dissolution applied to quartz

M. DELEUZE, A. GOIFFON, A. IBANEZ, E. PHILIPPOT

LPMS, URA D0407 CNRS, case 003, UM II, F-34095 Montpellier cédex, France

O. CAMBON

C.E.P.E, 44 Av de la Glacière, B.P. 165, F-95100, Argenteuil, France

Quartz chemical lapping of AT and SC cuts was performed in $\text{NaOH} \cdot x\text{H}_2\text{O}$ medium and this controlled dissolution resulted in reasonable quality of surface texture. Activation energy was calculated from dissolution rates measured against temperature. The initial surface texture of the samples influenced roughness parameter evolution but not the final roughness value. The electrical response of piezoelectric devices made by chemical lapping has been compared against others obtained by the IBE process. The comparison has shown that the controlled dissolution process is at least as good as IBE for producing piezoelectric devices.

1. Introduction

For quartz piezoelectric device manufacture, the crystalline quality of the material is of prime importance, and the atraumatic adjustment frequency of resonators is a very important step. Indeed, the Q -factor is closely related to both crystalline quality and the final surface roughness of the sample. Thus lapping must produce a good surface state, and a definite thickness which corresponds to the required frequency.

Unfortunately, for sophisticated high frequency resonators, with thickness less than $30 \mu\text{m}$, the mechanical lapping process cannot be used. Only the expensive ion beam etching technique (IBE) can be applied.

Much research has been devoted to another possibility, based on a chemical approach to these problems, using fluoride media [1–3], but has not resulted in an industrial method of quartz chemical etching being devised. Indeed, the HF or NH_4HF_2 baths used are very traumatic for the material, even with surfactants [4–6].

In our department, we have first defined the crystal growth conditions of a quartz-like material, AlPO_4 , berlinite in acid media, and its controlled dissolution in H_3PO_4 and H_2SO_4 [7, 8]. These two processes are closely related through the reverse thermodynamic relations [9–14], and these phenomena are even more controlled when experimental conditions are constituted by a solubility equilibrium, i.e. weak super- or under-saturation of solvents for crystal controlled growth or dissolution, respectively. In this case, an energy barrier, ΔG_d^* prevents most etch pit formation in the dissolution process, Fig. 1.

Taking into account these considerations, we investigated the quartz problem, which includes a factor critical for piezoelectric device manufacturing. The quartz crystal growth being made in a basic medium, our controlled dissolution has been carried out in a similar solvent, but inversely to the previous works [1–6]. Drastic growth conditions (high pressure and high temperature) were not applied, but these basic

media under standard conditions are rather atraumatic for the quartz. Indeed, it is a question of process reversibility: possible under certain conditions in a basic medium, but impossible in an acid one. We give here our first results for the two important wafer orientations: AT and SC cuts.

2. Experiments

2.1. Samples

We investigated two orientations in this work, AT and SC. All samples have been sawn from high- Q swept quartz bars. AT and SC discs of 5 to 12 mm in diameter were ground or polished. Two sizes of final abrasive were used: $3 \mu\text{m}$ for ground wafers and $0.3 \mu\text{m}$ for polished ones. The used plates were chosen in the range 800 to $67 \mu\text{m}$ thick before the chemical dissolution process. These thicknesses correspond to resonance frequencies ranging between 2 and 25 MHz. Therefore, the SC cuts were plano-convex plates.

2.2. Experimental procedure

2.2.1. Description of reactor

In this investigation, PTFE containers were used to avoid chemical corrosion of the $(\text{NaOH} + \text{H}_2\text{O})$ mixtures. Fig. 2 is an illustration of the apparatus used in basic medium.

2.2.2. Dissolution baths

Solutions were prepared from high purity sodium hydroxide pellets (MERCK pro analysis). Three different compositions were investigated: see Table I.

2.2.3. Measurement of plate thickness

The decrease in thickness of the wafers was checked during controlled dissolution by measurement of the resonance frequency given by :

$$F(\text{MHz}) = K(\text{MHz} \mu\text{m})/e(\mu\text{m})$$

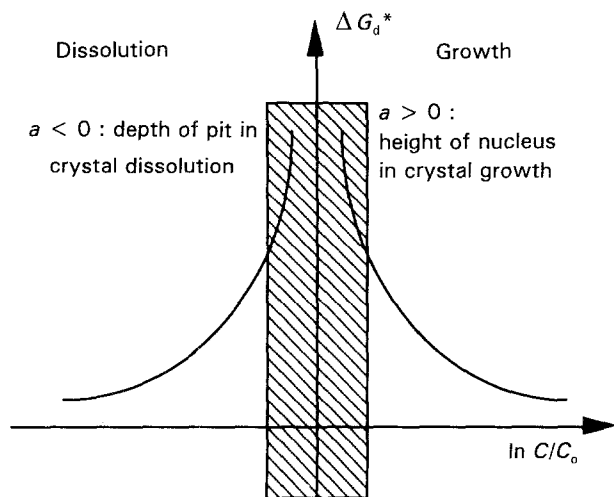


Figure 1 Schematic representation of the ΔG_d^* energy barrier variation for growth and dissolution of a real crystal in terms of solute concentration, C (C_0 = solubility at chosen temperature).

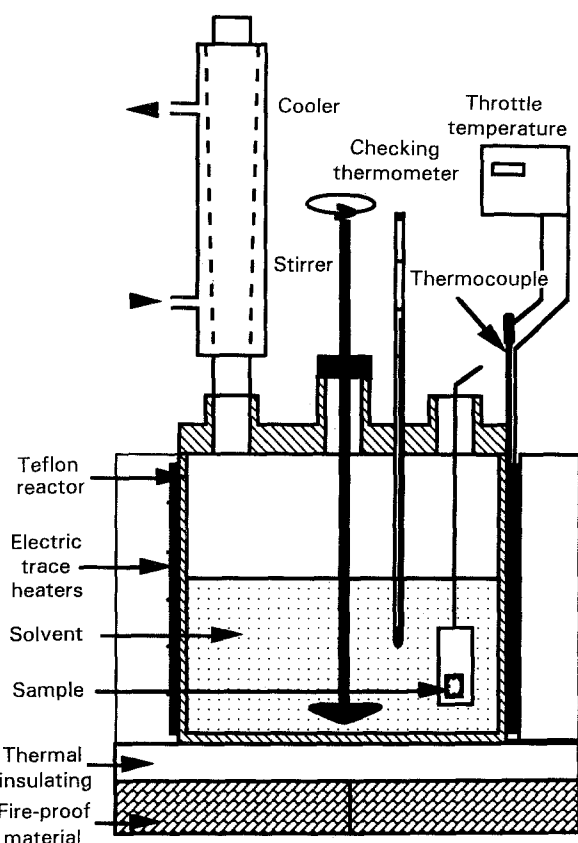


Figure 2 System used to thin down plates.

where e is the thickness of the plate and K is a constant related to the material and orientation studied. In the AT cut of quartz, $K = 1670 \text{ MHz } \mu\text{m}$ and $K = 1820 \text{ MHz } \mu\text{m}$ for the SC plano-convex plates. These measurements were made using a frequency meter which allows a broad range of frequencies from 0 to 110 MHz to be scanned.

2.2.4. Characterization of surface texture

Surface texture was examined using a Perthometer W5B surface profilometer. This apparatus, fitted with a microprocessor, was used to calculate the roughness

TABLE I Concentration of sodium hydroxide solutions for controlled dissolution

	Molality (mol kg^{-1} solvent)
NaOH·H ₂ O	55.6
NaOH·2H ₂ O	27.8
NaOH·3H ₂ O	18.5

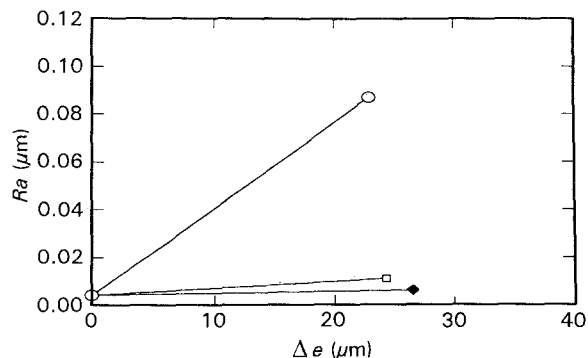


Figure 3 Change of roughness parameter for polished AT plates lapped by NaOH· $x\text{H}_2\text{O}$ (○ NaOH·3H₂O, □ NaOH·2H₂O, ◆ NaOH·H₂O).

parameter Ra (or average roughness) defined mathematically by the following equation:

$$Ra = \frac{1}{L} \int_0^L Z dx$$

where L is the profile length and Z is measured from the centre line, i.e. from the line so that the cross-section areas of asperities above and grooves below are equal. For reliability, all measurements were carried out with the same electric filter, $\lambda_c = 0.08 \text{ mm}$, and the given Ra value is the mean value of 4 different scanning directions (45° different from each other).

3. Results and discussion

3.1. Controlled dissolution of polished AT plates in NaOH· $x\text{H}_2\text{O}$ ($x = 1, 2, 3$) mixtures

The initial roughness value of the polished AT plates is $Ra = 0.004 \mu\text{m}$, which corresponds to an optical polished surface state. These first experiments, at 170°C , were undertaken to provide us with some knowledge on quartz behaviour in strongly basic conditions. The best solution seems to be the most concentrated one (Fig. 3). (Fig. 3 is only an illustration of these tests, Ra is not a linear function of the decrease in thickness Δe .) Indeed, for the more diluted medium, NaOH·3H₂O, the Ra value increases strongly from 0.004 to 0.09 μm after a thickness decrease of only 23 μm . Light microscopy observations ($\times 1100$) showed regular and oriented grooves.

On the other hand, for the most concentrated solvent, NaOH·H₂O, the roughness of the plates and their surface texture ($\times 1100$) did not differ from the initial values. For this reason, this last concentration was used to carry out the investigation of ground AT cut wafers in basic solutions.

Nevertheless, on an industrial scale, generally the wafers have a ground surface texture and, then, the determination of conditions for their good controlled dissolution is of great interest.

3.2. Controlled dissolution of ground AT plates in NaOH·H₂O mixtures

This controlled dissolution has been investigated in terms of several parameters: concentration of solvent, temperature of dissolution bath, and initial roughness of the wafer. From these results, dissolution kinetics of AT cut quartz in sodium hydroxide have been determined.

3.2.1. Influence of the solvent concentration

From preliminary investigation on polished samples, we have seen that dilution drastically affects the polishing properties of the sodium hydroxide medium. However, only two convenient concentrations have been used, i.e. the more concentrated ones: NaOH·H₂O and NaOH·2H₂O, to carry out the chemical dissolution of AT ground wafers. On the other hand, we checked if even more concentrated solutions improved the surface texture.

In Fig. 4, the roughness parameter evolution is the same for all three concentrations of the solvent and converges to the same, good value of $Ra \sim 0.05\text{--}0.06 \mu\text{m}$. Nevertheless, this decrease of Ra seems to be slightly less rapid for NaOH·2H₂O than for the other ones. This difference can be observed from light microscopy (Figs 5 and 6) where the etching figures are more accentuated for NaOH·H₂O medium. On the other hand, no significant improvement of the surface texture is registered for the more concentrated medium, NaOH·0.56H₂O.

Overall, the NaOH·H₂O medium is the best concentration for the chemical lapping of quartz AT cuts because both the other good media are limited by physical considerations: low boiling point for NaOH·2H₂O ($T_b \sim 158^\circ\text{C}$) and high melting point for NaOH·0.56H₂O ($T_m \sim 145^\circ\text{C}$).

3.2.2. Temperature influence

For this purpose, discs 6 μm in diameter were used

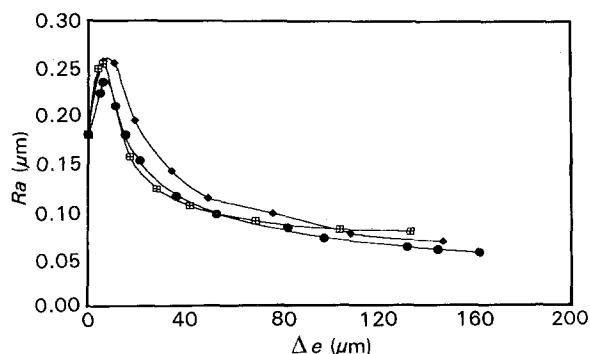


Figure 4 Roughness parameter Ra of AT plates plotted against removed depth for different sodium hydroxide concentrations (—●— NaOH·0.56H₂O 179°C, —□— NaOH·2H₂O 141°C, —●— NaOH·H₂O 166°C).

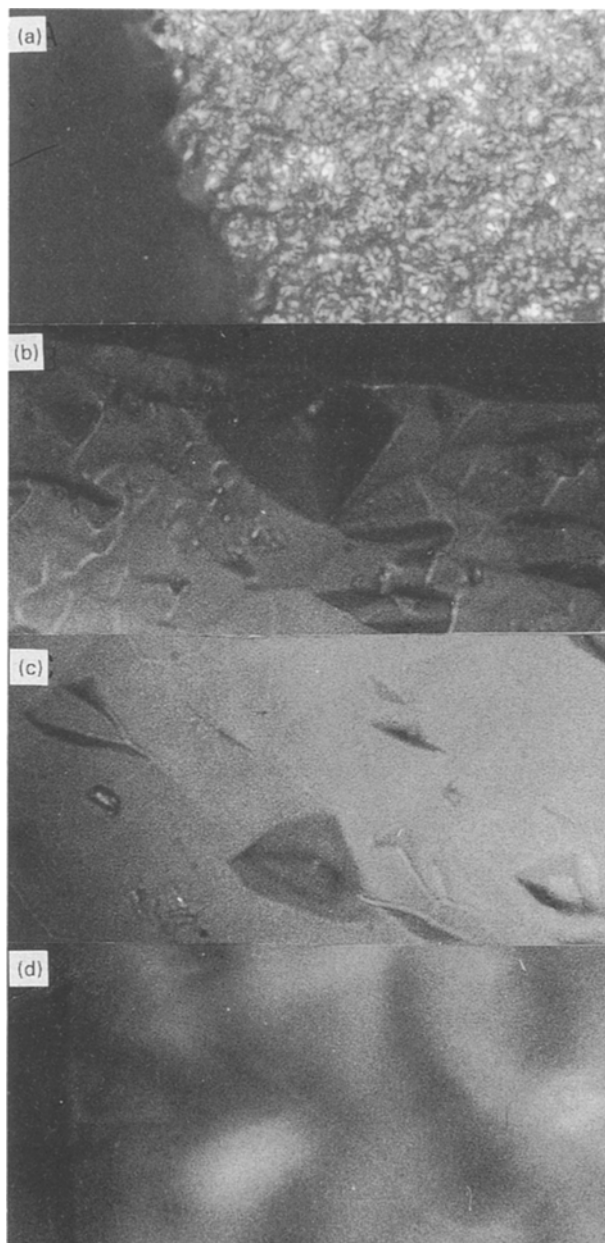


Figure 5 Photographs of AT cuts during the thinning down in NaOH·H₂O at 166°C. Magnification $\times 440$. (a) Prior to etching. (b) $\Delta e = 24 \mu\text{m}$. (c) $\Delta e = 40 \mu\text{m}$. (d) $\Delta e = 167 \mu\text{m}$.

with an initial frequency $\sim 10 \text{ MHz}$ ($e = 167 \mu\text{m}$) and a roughness value in the range $0.16 < Ra < 0.18 \mu\text{m}$. Some evolutions of the thinning down rates against the removed thickness have been plotted in Fig. 7.

As expected, these dissolution rates increased with temperature. All the curves, can be divided in two parts:

- the first part, related to a rapid decrease of the dissolution rate, corresponds to the chemical dissolution of the surface layer disturbed by cutting and polishing.
- in the second part, the dissolution rate becomes constant and is characteristic of the intrinsic dissolution rate for a given orientation of the material at the chosen temperature.

The first part corresponds to a total dissolution of $7 \mu\text{m}$, i.e. $3.5 \mu\text{m}$ per face. Of course, the same result can be found for the roughness parameter, from the curves Ra , plotted against the thinning down depth,

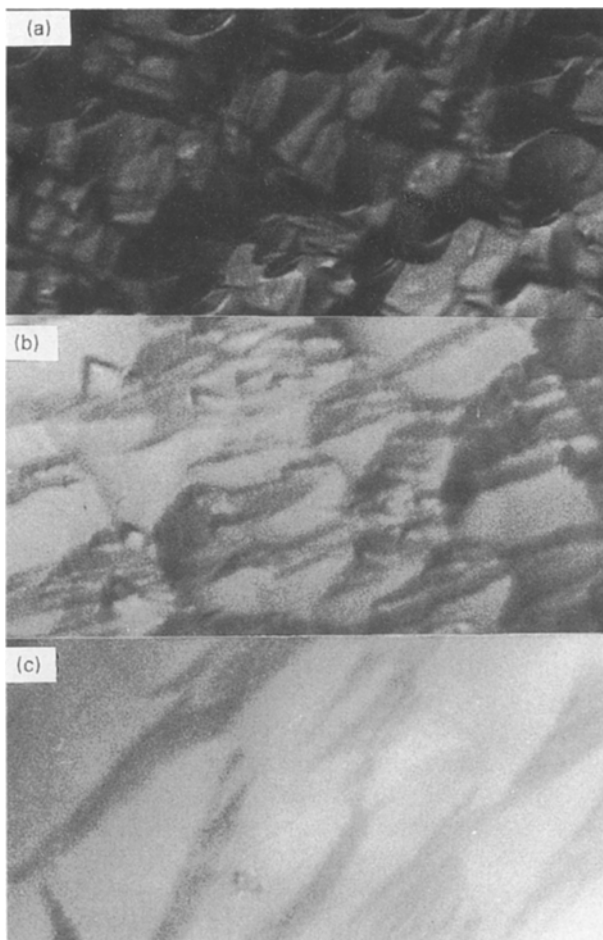


Figure 6 Photographs of AT cuts during the thinning down in $\text{NaOH}\cdot 2\text{H}_2\text{O}$ at 141°C . Magnification $\times 440$. (a) $\Delta e = 17\ \mu\text{m}$. (b) $\Delta e = 41\ \mu\text{m}$. (c) $\Delta e = 133\ \mu\text{m}$.

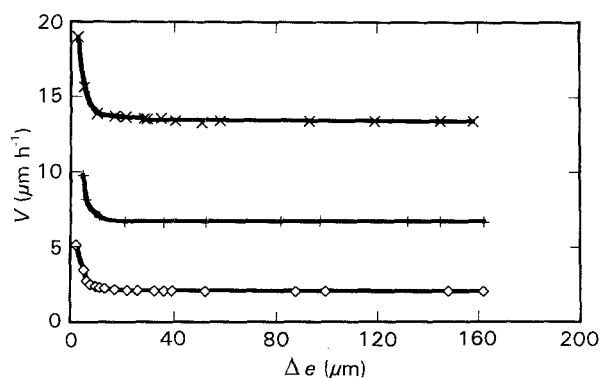


Figure 7 Dissolution rate V at different temperature of AT plates plotted against removed depth in $\text{NaOH}\cdot\text{H}_2\text{O}$ (\times — 178°C , $+$ — 166°C , \diamond — 146°C).

Δe , Fig. 8. Previous studies on quartz [15] and berlinite [7, 8] samples have already shown this behaviour.

Whatever the temperature, the $Ra = f(\Delta e)$ plots show a similar maximum for chemical lapping of about $7\ \mu\text{m}$ (for the two faces) and, then, slowly fall to a low value close to $0.06\ \mu\text{m}$, which corresponds to a good controlled dissolution of quartz material.

The surface texture evolution has also been checked by light microscopy, Fig. 5. First, the surface is formed by numerous disordered hillocks due to the disturbed superficial layer. Then, the maximum roughness value,

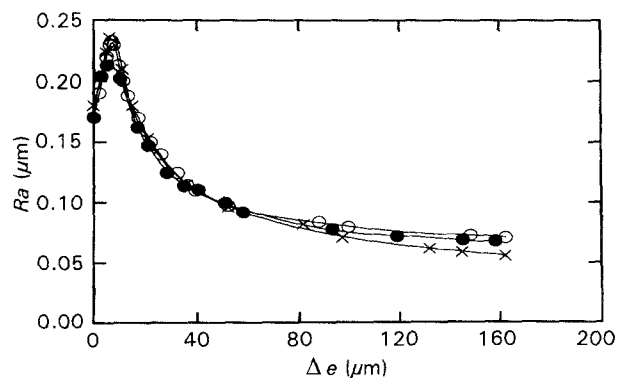


Figure 8 Roughness parameter Ra of AT plates plotted against removed depth in $\text{NaOH}\cdot\text{H}_2\text{O}$ (\circ — 146°C , \times — 166°C , \bullet — 178°C).

$Ra \sim 0.24\ \mu\text{m}$, obtained for removal of this superficial layer, corresponds to the true beginning of the crystal bulk dissolution. From this point, the polishing effect of the sodium hydroxide steadily improves the surface texture of the samples.

Since the roughness value stabilization was very slow, we tried to define the final Ra value after a longer chemical lapping time. Thus $630\ \mu\text{m}$ were removed from a $800\ \mu\text{m}$ thick wafer, and the Ra value decreased from 0.19 to $0.03\ \mu\text{m}$, and would certainly have continued to converge to a polished surface state. On the other hand, the isotropic effect of this thinning down process should be noted, which is evinced by no alteration in appearance of the circular shape of the quartz discs, even after removing several hundred micrometers.

In conclusion temperature has no effect upon the final roughness value of the chemical lapping, but only upon the thinning down rate.

3.2.3. Initial roughness (Ra_i) influence

From previous experiments in $\text{NaOH}\cdot\text{H}_2\text{O}$ medium, it appears that a slight change in the initial roughness of the wafers ($0.16 < Ra < 0.18\ \mu\text{m}$) corresponds to a slightly different final surface state, Fig. 9. Thus, it seems that the initial roughness influences the stabilization of the surface state in terms of removed depth. To investigate this several AT plates having different Ra_i values, Table II, were dissolved at 166°C .

The roughness evolution of these plates is plotted in Fig. 9. At first, we noted that the initial increase of Ra disappeared with the improvement of the surface state from 0.27 to $0.15\ \mu\text{m}$. We observed, however, that a low Ra value ($0.07\ \mu\text{m}$), was reached after a chemical lapping depth of only $40\ \mu\text{m}$ for sample 1 ($Ra_i = 0.15\ \mu\text{m}$). On the other hand, $160\ \mu\text{m}$ must be removed for sample 2 with worse initial roughness ($Ra_i = 0.18\ \mu\text{m}$) before reaching the same value. These results confirm previous research on quartz sample preparation [15, 16] and emphasize its importance for the chemical lapping process.

The effect of initial roughness is due to the slow polishing effect of the solvent used. Indeed, a high initial roughness corresponds to a thicker disturbed layer and leads to a more irregular bulk surface after

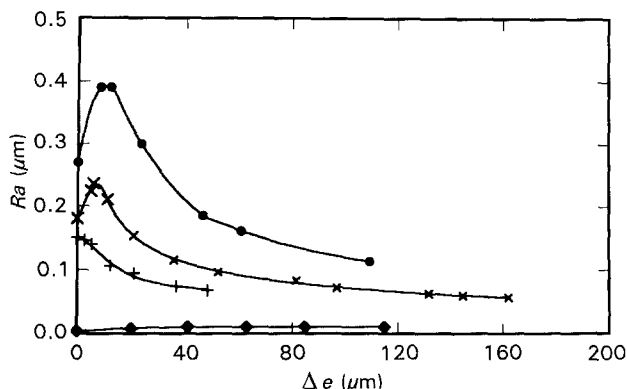


Figure 9 Roughness parameter R_a of different AT plates plotted against removed depth in $\text{NaOH}\cdot\text{H}_2\text{O}$ at 166°C (—+— plate 1, —*— plate 2, —●— plate 3, ◆ optical polished plate).

TABLE II Characteristics of AT plates dissolved at 166°C in $\text{NaOH}\cdot\text{H}_2\text{O}$

Plate	ϕ (mm)	Initial frequency (MHz)	R_{ai} (μm)
1	8	21	0.15
2	6	10	0.18
3	5	8	0.27
4	5	25	0.004

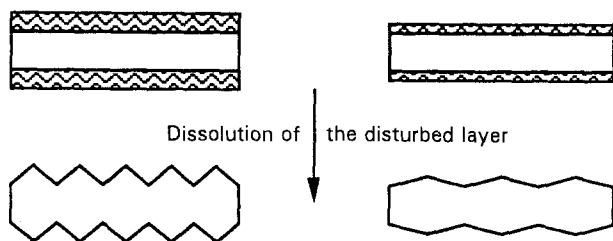


Figure 10 Schematic representation of crystal state under the disturbed layer.

the removal of this disturbed layer as schematized in Fig. 10. The thinning down, to reach the same surface state, will increase with initial roughness value.

In conclusion of the initial roughness influence, the improvement of quartz AT plate roughness is significantly accelerated using a smoother surface state for the controlled dissolution process.

3.2.4. Dissolution kinetics of AT quartz plates in $\text{NaOH}\cdot\text{H}_2\text{O}$ and $\text{NaOH}\cdot 2\text{H}_2\text{O}$

The evolution of dissolution rate against temperature is plotted in Fig. 11. Since the chemical lapping rate is strongly influenced by temperature, this parameter must be carefully checked during the adjustment of the resonator frequency. The exponential variation corresponds to a thermally activated mechanism, following Arrhenius's law:

$$kT = A \exp(-E_a/RT)$$

kT being directly related to the thinning down rate, E_a can be calculated from:

$$\ln(V) = f(1/T)$$

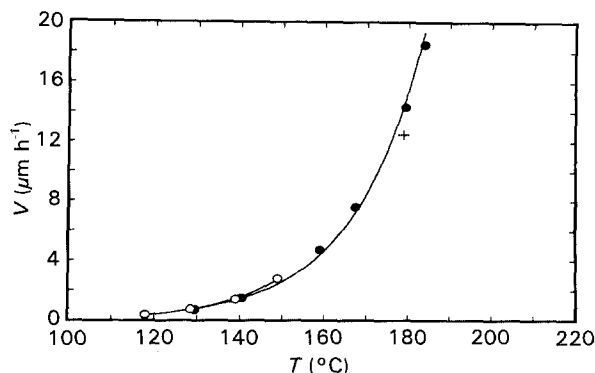


Figure 11 Dissolution rate of AT plates in $\text{NaOH}\cdot x\text{H}_2\text{O}$ versus temperature (+ $\text{NaOH}\cdot 0.56\text{H}_2\text{O}$, —●— $\text{NaOH}\cdot\text{H}_2\text{O}$, —○— $\text{NaOH}\cdot 2\text{H}_2\text{O}$).

with

$$V = A' \exp(-E_a/RT)$$

where V = thinning down rate in $\mu\text{m h}^{-1}$, E_a = activation energy in kJ mol^{-1} and A' = the pre-exponential term including the frequency factor A and the solution concentration. Indeed, the variation of $\ln(V)$ against $1/T$ is a straight line. This graph determines the E_a value. Thus the activation energy corresponding to this dissolution process is $E_a = 91 \text{ kJ mol}^{-1}$ for $\text{NaOH}\cdot\text{H}_2\text{O}$ and 88 kJ mol^{-1} for $\text{NaOH}\cdot 2\text{H}_2\text{O}$.

The low boiling point of $\text{NaOH}\cdot 2\text{H}_2\text{O}$ ($\sim 158^\circ\text{C}$) does not allow the use of this solvent under this temperature, and thus we can only measure the dissolution rate. In this field, the dissolution rate is not very affected by temperature and, so, it is difficult to determine the small difference between the two dissolution rates. Therefore, only a few values are available to calculate the activation energy, so, the error must be more important than for $\text{NaOH}\cdot\text{H}_2\text{O}$.

Nevertheless, we can say that the dilution of solvent affects the dissolution rate; in fact, the dilution increases kinetics but limits the usable temperature range.

3.2.5. Conclusion for controlled dissolution of quartz ground AT cuts

From all these results, the best conditions for the controlled dissolution of quartz AT cut plates seem to be the $\text{NaOH}\cdot\text{H}_2\text{O}$ medium. The dissolution process corresponds to a thermally activated mechanism where temperature has no effect upon the final surface state, but only upon the dissolution rate, and where the initial roughness of the sample can strongly modify the rate of improvement of the plate roughness.

This study has been extended to other plate orientations, and chiefly to the double-rotated SC plates which are widely used on an industrial scale.

3.3. Controlled dissolution of quartz SC cut in $\text{NaOH}\cdot\text{H}_2\text{O}$

Many works [17–20] have shown the drastic influence of the wafer crystallographic orientation on the

dissolution characteristics, and then, the SC cut behaviour in this solvent has been investigated. All the initial experiments have been carried out in $\text{NaOH}\cdot\text{H}_2\text{O}$ solvent which is the best one for the AT cut.

3.3.1. Controlled dissolution of polished SC plates in $\text{NaOH}\cdot\text{H}_2\text{O}$

As for the AT study, first the dissolution process of polished wafers was investigated in soda and the results are summarized in Table III. All the plates were thinned down at 174°C and the surface state evolution was controlled. The maximum R_a value, obtained after $174\ \mu\text{m}$ was removed, was $0.01\ \mu\text{m}$ which corresponded to an optical polished surface state. Meanwhile, for all tests, etch pits began to appear on one side of the plate after $\sim 60\ \mu\text{m}$ was removed (after that, the R_a value does not take into account these etch pits).

3.3.2. Controlled dissolution of ground SC plates in $\text{NaOH}\cdot x\text{H}_2\text{O}$

For this purpose, discs 9 mm in diameter were used with an initial roughness value close to $0.11\ \mu\text{m}$.

As for the AT cut dissolution (Fig. 7), the thinning down rate was constant after an initial rapid decrease due to the superficial disturbed layer. The evolution of the surface texture against the chemical thinning down is plotted in Fig. 12. The R_a evolution sets out a drastic difference between two faces, as can be observed in Fig. 13, but converges to the same final roughness value, $R_a \sim 0.06\ \mu\text{m}$.

TABLE III Characteristics of SC polished plates thinned down by $\text{NaOH}\cdot\text{H}_2\text{O}$

Plate	Initial R_a (μm)	Δe (μm)	Final R_a face 1 (μm)	Final R_a face 2 (μm)
1	0.005	21.9	0.008	0.008
2	0.005	11.7	0.008	0.008
3	0.005	9	0.006	0.006
4	0.005	62	0.008	0.008
5	0.005	174	0.01	0.01

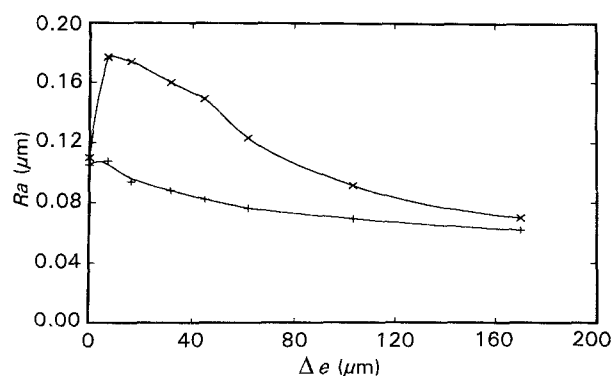


Figure 12 Roughness parameter R_a of the two sides of a SC plate plotted against removed depth in $\text{NaOH}\cdot\text{H}_2\text{O}$ (—+— R_a side 1, -x- R_a side 2).

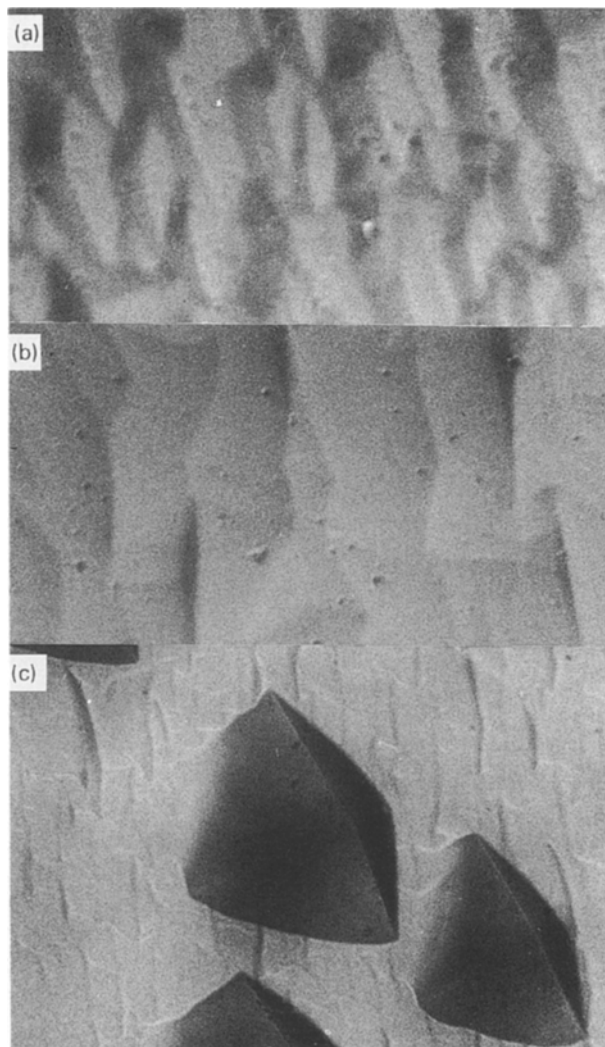


Figure 13 Photographs of the two sides of SC cut in $\text{NaOH}\cdot\text{H}_2\text{O}$ at 174°C . Removed depth = $206\ \mu\text{m}$. (a) Side one magnification $\times 440$. (b) Side two magnification $\times 440$. (c) Side two, dissolution figure, magnification $\times 110$.

Unfortunately, as for the polished SC wafers, some etch pits begin to appear, only on one side of the plate (on the roughest face), after $60\ \mu\text{m}$ removal, Fig. 13 (the R_a parameter does not include these etch pits). If the thinning down is extended to $206\ \mu\text{m}$ depth, the R_a value converges to $0.05\ \mu\text{m}$ for the both faces (out of etch pits).

3.3.3. Dissolution kinetics of quartz SC-cuts in $\text{NaOH}\cdot\text{H}_2\text{O}$

The dissolution rate of SC plates in sodium hydroxide against temperature is plotted in Fig. 14. Its exponential variation corresponds to a thermally activated mechanism, as found for AT plates. The activation energy $88\ \text{kJ mol}^{-1}$ is close to the value found for AT plates.

3.3.4. Conclusion for controlled dissolution of quartz SC cuts

From this preliminary study, the polishing effect of $\text{NaOH}\cdot\text{H}_2\text{O}$ medium for SC cuts seems not to be as good as for AT cuts. Indeed, the appearance of some

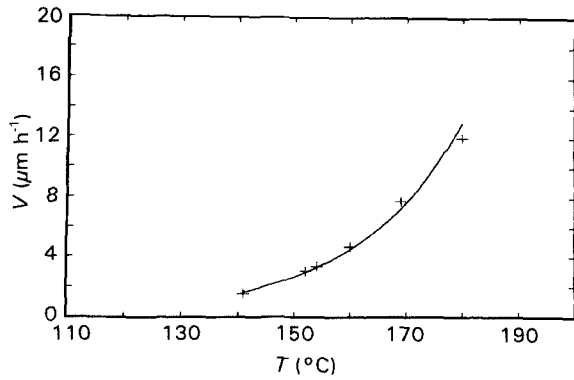


Figure 14 Dissolution rate V of SC plates in $\text{NaOH}\cdot\text{H}_2\text{O}$ versus temperature.

large etch pits, distributed over one whole side of the sample, does not allow its use for a prolonged thinning down. Most probably, the etch pit formation must be favoured by crystal defects such as dislocations.

3.4. Comparison of dissolution process between AT and SC cuts

As already noted [17–20], the controlled dissolution process of quartz plates is drastically related to their crystallographic orientation. Drastic differences can appear, as well, in kinetics such as in smoothing, even for both sides of the same sample (SC cut), Figs 12 and 7.

For the single rotated AT cut, a 2-fold axis is lying in the wafer and, this explains the symmetry of dissolution motive for both sides of the wafer. Now, for double rotated SC cut, the absence of a 2-fold axis gives different dissolution motives and surface texture for both sides of the sample.

For the activation energy of the dissolution processes, they are equal in the range of their calculated relative error, $\sim 6\%$ (91 and 88 kJ mol^{-1} for AT and SC cuts, respectively in $\text{NaOH}\cdot\text{H}_2\text{O}$). Thus, this dissolution process must follow the same thermally activated mechanism.

In conclusion, $\text{NaOH}\cdot\text{H}_2\text{O}$ seems to be the best sodium hydroxide concentration for controlled dissolution of quartz AT and SC cuts. Unfortunately, results have yet to be improved for prolonged thinning down of SC wafers.

From these studies, first resonators have been realised by chemical lapping of AT cuts and initial results of their piezoelectric characteristics are given in the last section.

4. Piezoelectric characterization of resonators made by chemical lapping

To check the efficiency of the chemical lapping process, piezoelectric devices were produced after the controlled dissolution of AT quartz plates. In a first step, some high frequency AT resonators were tested to check their Q -factor and the reproducibility of the process. Then, four resonators were chosen to test a four-pole bandpass linear-phase filter.

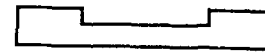


Figure 15 Well plate.

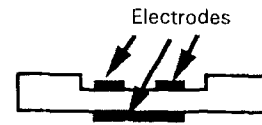


Figure 16 Two-pole resonator.

TABLE IV Reproducibility of the dissolution rate for five different wafers. The final frequency can be achieved with one or several thinning down steps

Plate	Time (min)	Initial frequency (MHz)	Final frequency (MHz)	Removed depth (μm)
1	85	49.31	84.56	14.1
2	85	49.33	84.63	14.1
3	85	49.37	84.63	14.1
4	83	49.71	84.72	13.9
5	85	49.32	84.57	14.1

TABLE V Electrical parameters of resonators obtained from controlled dissolution and IBE processes

	Resonators	
	IBE	Chemically lapped
F_r (kHz)	82873	82870
R (Ω)	28.59	27.02
L (mH)	2.894	3.3721
Q	52710	65000
$Q \cdot F_r$	4.37×10^{12}	5.38×10^{12}

4.1. Sample preparation

The objective was to realize 83 MHz resonators after metallization, i.e. 84.5 ± 0.2 MHz before metallization (in fundamental mode). The final thickness of these samples, ~ 20 μm, required a stiffening of the external part of the plate by boring a central well, Figs 15 and 16.

Controlled dissolution of these plates was performed in sodium hydroxide solutions at 170 °C with a dissolution rate near 10 μm h^{-1} for both sides of the wafer. Table IV summarizes the main results for five different wafers.

4.2. Piezoelectric characterizations

Two kinds of measurements were used:

Air-gap method: The air gap method is a technique well adapted to the chemical lapping process because sample measurements can be made without adherent metallic electrodes. Some results from this method are given in Table IV, where all measurements are in the predetermined range, 84.5 ± 0.2 MHz.

Resonator measurements: For two-pole resonators, metallic electrodes are deposited on the two faces of the plates by an evaporation technique and connected to a network analyser. Table V and Fig. 17 summarize

TABLE VI Electrical parameters and specifications of linear-phase filters

Specifications		Filters	
		Chemically lapped	IBE
F_c (kHz)	83000	82986	83005
BW (kHz) at 3 dB	180	200	213
IL (dB)	5.5	3.9	3.0
25 dB	$F_c \pm 200.0$	+ 175.0 - 183.8	$\approx \pm 180$
40 dB	$F_c \pm 285.0$	+ 252.9 - 252.9	$\approx \pm 260$
50 dB	$F_c \pm 1000.0$	+ 312.5 - 306.3	$\approx \pm 330$
Out of band attenuation (dB)	60 dB at ± 30.0 MHz	- 87.3 + 89.0	> 80 dB

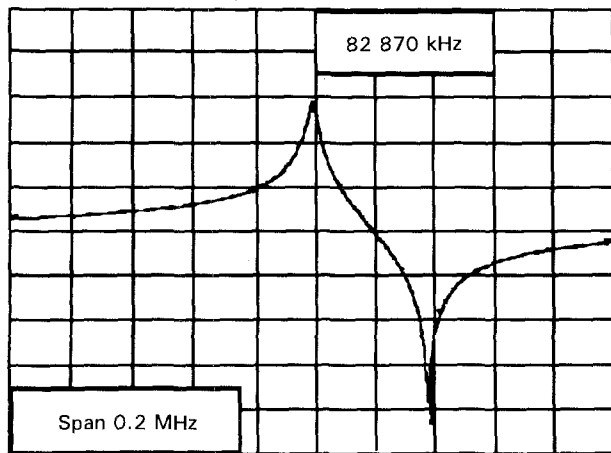


Figure 17 Frequency response of resonator with plates chemically thinned down.

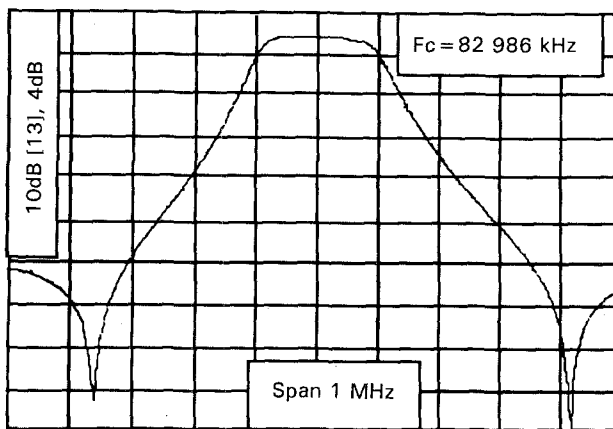


Figure 18 Linear phase filter manufactured with chemically thinned down plates.

comparative characteristics of the resonators obtained from controlled dissolution and IBE processes. From these initial results, the more traumatic chemical lapping seems to give specifications as least as good as those of the ion beam etching.

In a last step, four-pole linear-phase filters were made from two chemically lapped resonators and two IBE ones. These filters were characterized by a frequency response which must be in the range of specification defined by:

(a) a bandwidth for a maximum insertion loss (IL) allowed: A_{max} .

(b) an attenuated band for a minimum insertion loss allowed: A_{min} .

The characteristics of these filters are given by F_c , central frequency, BW , bandwidth at n dB and Ba , attenuated band at n dB. Thus, these linear-phase filters are also characterized by a constant propagation time t (delay) in a part of bandwidth. Filter characteristics and specifications are given in Table VI, and frequency response in Fig. 18.

The characteristics here also confirm the attraction of an atraumatic controlled dissolution process [21]. These piezoelectric results show that the surface state reached is sufficient for BAW devices to be made.

5. Conclusion

From previous works [9-14], it appears that crystal growth and crystal dissolution are controlled by the same laws and, thus, we have investigated the chemical lapping of quartz in sodium hydroxide which is used in its crystal growth process, although dissolution conditions are far from the crystal growth ones. In other terms, dissolution is a reversible phenomenon under certain conditions, whereas the etching agent commonly used, F^- , involves an irreversible chemical reaction.

Consequently, the word "etching" has never been used in this paper to avoid all confusion with the "controlled dissolution". From our point of view, the etching term must be reserved for irreversible processes such as quartz in fluoride media. On the other hand, the controlled dissolution implies that the phenomenon can be reversible, such as quartz in basic solvents.

So, chemical lapping of AT and SC quartz cuts have been investigated in basic solvents. Then, conditions giving a good surface state with a definite thickness, in agreement with the required frequency, have been specified for AT and SC cuts in sodium hydroxide. Although the good results for AT cuts are beginning to be transferred to an industrial scale [21], conditions for SC cuts must still be improved

Acknowledgements

The authors wish to thank C. N. R. S. and C. E. P. E./Thomson for their financial support.

References

1. K. BRÄUER and E. MÜLLER, *Cryst. Res. Technol.* **19** (1984) 101.
2. K. H. JONES, in Proceedings of the 41st Annual Frequency Control Symposium (1987) p. 199.
3. C. R. TELLIER, *Surf. Technol.* **21** (1984) 83.
4. A. J. BERNOT, in Proceedings of the IEEE Frequency Control Symposium (1985) 271.
5. R. J. BRANDMAYR and J. R. VIG, in Proceedings of the 39th Annual Frequency Control Symposium (1985) 273.
6. *Idem*, in Proceedings of the 40th Annual Frequency Control Symposium (1986) 86.
7. O. CAMBON, A. GOIFFON, A. IBANEZ and E. PHILIP-POT, *J. Solid State Chem.* **103** (1993) 240.
8. *Idem*, in Proceedings of the 6th European Frequency and Time Forum (1992) 377.
9. J. FRENKEL, *J. Phys. USSR* **9** (1945) 392.
10. W. K. BURTON, N. CABRERA and F. FRANK, *Nature* **163** (C 1949) 398.
11. *Idem*, *Phil. Trans. Soc. London* **243** (C 1951) 299.
12. P. BENNENA and G. H. GILMER, *J. Cryst. Growth* **13** (1972) 148.
13. W. G. JOHNSTON, *Prog. Ceram. Sci.* **2** (1962) 1.
14. N. CABRERA and N. LEVINE, *Phil. Mag.* **1** (1955) 450.
15. C. R. TELLIER and J. L. VATERKOWSKI, *Surf. Technol.* **15** (1985) 275.
16. Y. SEKIGUCHI and H. FUNAKUBO, *J. Mater. Sci.* **15** (1980) 3066.
17. C. R. TELLIER, F. JOUFFROY and F. C. BURON, *Master. Chem. Physics* **14** (1986) 25.
18. C. R. TELLIER, in Proceedings of the IEEE Frequency Control Symposium (1985).
19. J. R. HUNT, in Proceedings of the 41st Annual Frequency Control Symposium (1987).
20. C. R. TELLIER and F. JOUFFROY, *J. Mater. Sci.* **18** (1983) 3621.
21. Patent 07/19/1991 Ref. 9109170, European Patent No. 2679225.

*Received 11 August 1993
and accepted 21 March 1994*